Design Methodology of a Multi-village Microgrid

Case Study of the Sahel Region

Nouhou Bako Z.***, Abdou Tankari M.*, Seidou Maiga A.**, Lefebvre G.*

*CERTES Lab., University of Paris-Est Creteil, 61, Av. du Général De Gaulle, 94010, France

**EITER Laboratory, Gaston Berger University, BP 234 Saint-Louis, Senegal

***University Dan Dicko Dankoulodo of Maradi, BP 465 Maradi – Niger

zeinabou.bako@uddm.edu.ne, mahamadou.abdou-tankari@u-pec.fr

Received: 17.03.2018; Accepted:23.03.2018

Abstract- This paper deals the optimal sizing and location of the power plant in a microgrid interconnecting several villages. The case study is defined by eight villages of rural community of Dakoro, in Niger. The methodological approach proposed is based on a matrix of distances established from the geographical coordinates of the sites. This serves as a basis for the estimation of the losses as well as for estimation of the shortest path defining the architecture of the microgrid. The energy requirement is then estimated for sizing power sources (PV, diesel generator) and energy storage units. The particle swarm optimization method is applied to the data with some criteria and constraints. The proposed energy flow management strategy is tested on a realtime system according to different scenarios. The results are presented and analyzed.

Keywords Microgrid, multi-village, optimal location, photovoltaic, battery, diesel generator, cost of electricity, shortest path, graph theory, particle swarm optimization.

1. Introduction

Global warming is manifesting itself more and more around the world in different forms such as droughts, famines, high temperatures and floods. This results in significant economic, societal and environmental impacts. Its main causes are energy-consuming lifestyles and a strong use of fossil fuels. Palliative measures are necessary to preserve the environment and the health of the populations. It is therefore urgent to change the mode of energy production and consumption, to reinforce the energy efficiency of the systems and to develop the energy mix.

For these reasons, all countries of the world are invited to start a strong and urgent energy transition. Africa countries are also concerned, although their rate of access to electricity is very limited. Around 1.2 billion people in the world do not have access to electricity. In Africa, the access rate is around 30% but with a significant disparity between urban (89% of the urban population) and rural (46% of the rural population) [1] [2]. The access to electricity with good quality is a major challenge for the countries of sub-Saharan Africa. It can be observed a very low rate of access in rural areas, less than 5%, compared to that urban area ones, of about 40% [1]. These countries, where the energy coverage is also low, intend to improve the penetration ratio of the renewable energy from 5% in 2013 to 22% in 2030 in Africa, by developing micro-electrical networks.

This paper proposes a design methodology of multi-source systems supplying a micro-grid of several interconnected villages. The main challenges are to study the characteristics of the villages and the energy demand, to master the constraints and to develop a sizing and decision-making tools. For this, eight villages in the rural district of Dakoro, in Republic of Niger, are considered in the case study.

The characteristics of the villages are studied in aims to analyze their spatial distribution, to define their distances matrix, and to estimate the climatic conditions (solar radiation, temperature). Then, a methodology of energy demand estimation is presented before to detail the strategy of energy management in the multi-sources system. The proposed method uses sizing models of the system and it is based on a power flow strategy associated to the particle swarm swarm optimization method. Experimental tests are performed to validate the power flow management strategy before using it for optimal power plant design and location. The cost of electricity is estimated by using the PSO (Particle Swarm Optimization) method that minimizes the proposed objective function.

2. Characteristics of the Study Area

2.1. Spatial Distribution of Villages

The rural community of Dakoro covers 42.8% of the area of the Maradi region, in the Republic of Niger. The two main

activities of the people are the pastoralism (9 months) and agriculture (3 months). The density of its population, estimated around 34 people per square kilometer, is the lowest of the Maradi region. Part of its population is nomadic and the villages are sparse. Thus, the strong demographic growth, the dispersion of the villages, and the nomadism of a part of the population are the parameters to take into account in the management strategy of the energetic demand in social services.

2.1.1. Villages location

The study area is defined by eight villages of Dakoro, presented in Fig.1. They are interconnected through a microgrid whose architecture is defined from the knowledge of locations (GPS coordinates, distances) of all the villages to feed. To compensate for the lack of climatic measurement data, online or offline computer tools can be used to map, locate and record data about the target villages. Different configurations of the microgrid are possible, each with its constraints, advantages and disadvantages.

In this study, a centralized power production is considered to be located at the village with the optimal position. This facilitates monitoring and daily maintenance. It can avoid the accessibility difficulties that can arise in the case of regular maintenance activities. Nevertheless, the networking of feed villages requires regular monitoring of transmission lines, based on a SCADA system that can ensure monitoring and incident detection.

2.1.1. Shortest Path based Microgrid Architecture

The short-path methods, inspired by graph theory, are applied in order to estimate the minimal links defining the optimal architecture of the multi-source multi-village system. The minimum spanning tree connecting all the villages to each other is determined by applying Prim's theorem to the location data of the villages. The distances corresponding to the shortest path connecting all villages are colored in bold in Table 1. The result is illustrated in Fig. 2. This configuration achieves the minimum total length and therefore the minimum of power losses compared to other possible links.

On the other hand, for the same architecture, the losses vary according to the powers flow between the villages. It therefore becomes necessary to determine the best location of the microgrid plant that achieves the minimum energy losses.

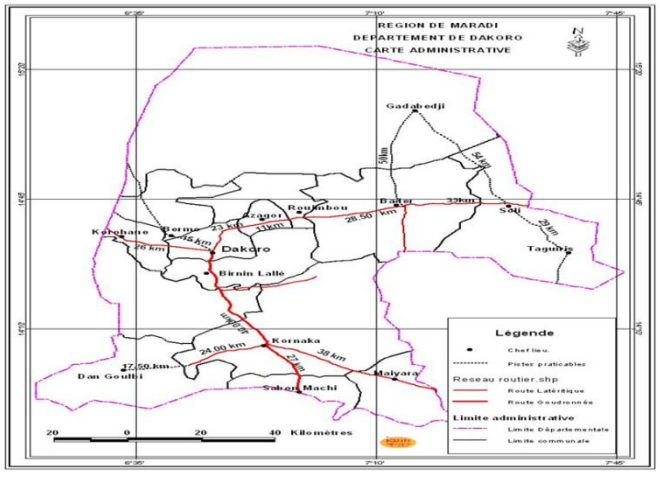

Fig.1 : Cartographie de la commune de Dakoro

Table 1. Distances between villages (km) – shortest path is defined by bold red points with total length of 190,52km

Village	1	2	3	4	5	6	7	8
1	0	**11.45**	**27.5**	**18.89**	84.46	43.39	60.98	87.29
2	11.45	0	38.42	28.31	91.24	54.69	63.34	88.43
3	27.5	38.42	0	28.31	84.21	**17.46**	73.8	100.76
4	18.89	28.31	28.31	0	66.31	36.63	**47.56**	74.58
5	84.46	91.24	84.21	66.31	0	79.51	40.61	46.34
6	43.39	54.69	17.46	36.63	79.51	0	77.73	103.82
7	60.98	63.34	73.8	47.56	**40.61**	77.73	0	**27.05**
8	87.29	88.43	100.76	74.58	46.34	103.82	27.05	0

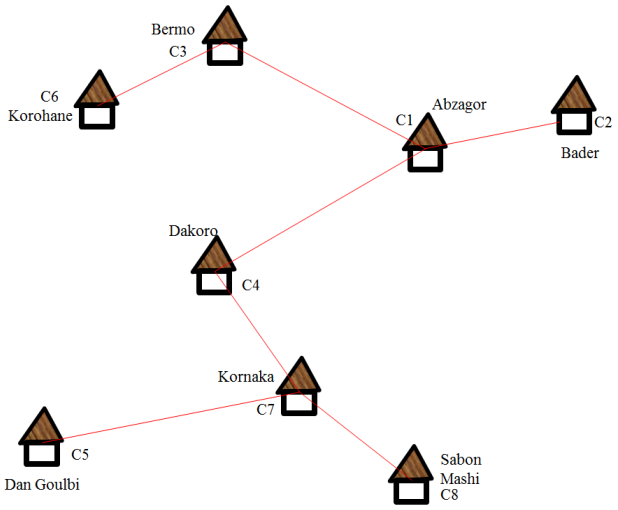

Fig.2 : Shortest path between all villages corresponding to the microgrid architecture

2.1.2. Estimation of solar radiation

The efficient use of a solar PV system depends on the solar radiation characteristics of the PV system location, obtained from experimental measurements. But, the measuring instruments are not available in some parts of the world because of their purchase cost, maintenance and also calibration [3], [4]. Generally, in weather stations, global solar radiation is measured on horizontal surfaces. The available data are limited to empirical measurements of monthly mean values of sunlight (measurement by heliograph). These are often extrapolated, with a lot of inaccuracy, from the mean daily data.

The daily PV production depends on the date, the time of day, the duration of exposure, the actual daily irradiation duration, and also on the inclination and orientation of the panel [5]. The prediction of the optimum production, for a given village, requires the knowledge of the zenith angles and of the solar radiation components (direct, diffuse and total horizontal).

Many studies show that the orientation and inclination have a strong influence on the maximum energy produced by the PV generator. Several methods for determining the optimal angle according to seasons and climate variations are proposed in [4], [6], [7], [8] - [21]. Long terms hourly data of sunshine are necessary during the system sizing step, to take into account the hourly variability of the climatic conditions, but also during the real operation in order to realize

permanently an effective supervision based on the system history. At the control level, real-time measurements are performed to adapt the operation to high variability and to ensure the continuous maximum power point tracking (MPPT).

The hourly value H_t of the solar radiation in the plane of the PV panel, as well as its daily hourly mean $\overline{H}_t$,, is defined by (1). It is a function of the soil albedo ρ, the angle of incidence θ as well as the zenith angle of the sun θ_z. For a monthly average temperature of the village lower than (-5 ° C), the albedo is fixed at 0.7. If the temperature is above (0°C), the albedo is set at 0.2. Between (-5°C) and (0°C), it is estimated by linear interpolation.

$$\begin{cases} H_t = H_b \frac{cos\theta}{cos\theta_z} + H_d \left(\frac{1+cos\beta}{2}\right) + H\rho \left(\frac{1+cos\beta}{2}\right) \\ \overline{H}_t = \frac{\sum_1^{24} H_t}{24} \end{cases} \quad (1)$$

Let's define $\overline{H}$ as the monthly mean values of global daily sunlight, $\overline{H}_b$ as its direct component, emitted by the solar disk and $\overline{H}_d$ as its diffuse component, emitted by the rest of the celestial vault. The instantaneous values are defined as the global horizontal sunlight *H* with its diffuse H_d and direct H_b components. The relations between these parameters are expressed by (2), from the formulas of Collares-Pereira and Rabl for the global radiation and the formula of Liu and Jordan for diffuse radiation.

$$\begin{cases} H = \frac{\pi}{24} * \frac{cos\omega - cos\omega_s}{sin\omega_s - \omega_s cos\omega_s} * (a + b * cos\omega) * \overline{H} \\ H_d = \frac{\pi}{24} * \frac{cos\omega - cos\omega_s}{sin\omega_s - \omega_s cos\omega_s} * \overline{H}_d \\ H_b = H - H_d \end{cases} \quad (2)$$

with,

$$\begin{cases} a = 0{,}409 + 0{,}5016 * sin\left(\omega_s - \frac{\pi}{3}\right) \\ b = 0{,}6609 - 0{,}4767 * sin\left(\omega_s - \frac{\pi}{3}\right) \end{cases} \quad (3)$$

The hour angle ω, in radians, is positive during the morning. It becomes zero at solar noon and negative as the afternoon progresses. In particular cases of sunrise and sunset, there are the same numerical value of hour angle, expressed as ω_s, but the sunrise angle is negative and the sunset angle is positive sign. The correlation of Erbs et al. [22] is used to calculate the diffuse component $\overline{H}_d$ based on the monthly average of a daily sunlight (4), according to a monthly average of the clarity index $\overline{K}_T$, varying from 0.3 (rainy regions or seasons) to 0.8 (dry and sunny seasons). Outside this range, a linear interpolation is performed.

$$\frac{\overline{H}_d}{\overline{H}} = \begin{cases} 1{,}391 - 3{,}560\overline{K}_T + 4{,}189\overline{K}_T^2 - 2{,}137\overline{K}_T^3, \ if\ \zeta < 81{,}4° \\ 1{,}311 - 3{,}022\overline{K}_T + 3{,}427\overline{K}_T^2 - 1{,}821\overline{K}_T^3, \ if\ \zeta > 81{,}4° \end{cases} \quad (4)$$

The clarity index $\overline{K}_T$ is estimated from the average of the extraterrestrial radiation $\overline{H}_0$ (5), which instantaneous value on a horizontal surface H_0 is the solar radiation before it reaches the atmospheric layer, of the day *n*. It is attenuated by the atmosphere and the clouds in proportion to the clarity index K_T. The solar constant G_{cs} is estimated at 1367W/m², with *m*=28 ; 30 or 31 days of the month. The declination δ, angle of the sun at the maximum of its course (solar noon), is estimated by (7), in degree. The day of the year n = 1 corresponds to the 1st of January, and n = 32 to the 1st day of February. The declination varies between -23.45 ° and +23.45, corresponding to December 21th and June 21th respectively.

$$\begin{cases} H_0 = \gamma * \frac{86400 G_{cs}}{\pi} * \left(1 + 0{,}033 cos\left(2\pi \frac{n}{365}\right)\right) \\ \overline{H}_0 = \frac{\sum_1^m H_0}{m} \\ \overline{K}_T = \frac{\overline{H}}{\overline{H}_0} \end{cases} \quad (5)$$

$$\gamma = (cos\psi cos\delta sin\omega_s + \omega_s sin\psi sin\delta) \quad (6)$$

The declination and the latitude ψ are used to estimate the hour angle of the sun, which is the angular displacement of the sun around the polar axis in its moving from East to West, with respect to the local meridian. It is zero at solar noon, negative in the morning, positive in the afternoon and increases by 15° per hour, to achieve a 360° turn in 24 hours. The sun's angle at sunrise and sunset is called the hourly sun angle ω_s (7).

$$\begin{cases} \omega_s = Arccos(-tan\psi tan\delta) \\ \delta = 23.45 sin\left(2\pi \frac{284+n}{365}\right) \end{cases} \quad (7)$$

2.2. Estimation of energy demand

Depending on usage, access to energy services can be classified into three levels. The first level of access to energy concerns households and the satisfaction of basic human needs through water pumping, lighting, education, health and communication. The second level allows productive uses based on the development of economic and productive activities such as trade, transport, and agriculture. The third level corresponds to meeting the individual and collective needs of so-called modern societies through individual and collective needs such as refrigeration, heating and sanitation [23].

3. Energy Management Strategy

3.1 Multi-source sizing models

An autonomous micro-grid of Fig.3 must ensure permanent energy availability. To do this, an information layer is added to the power layer in order to achieve effective management in real time, through continuous monitoring and responsiveness in the event of faults. The information layer integrates different features such as network of various sensors, system of data acquisition and storage (SCADA), local control of electronic converters, global supervision and decision rules, interfaces and information flow media (internet, radio frequency, cable, satellite, …). The strategy of the optimal sizing of the multi-source system is presented in the flowchart of Fig.4.

3.2 PV power production

The electrical energy available at the output of the PV panel is given by the following well known expression (8).

$$\begin{cases} E_A = \eta_p \eta_r (1 - \lambda_p)(1 - \lambda_c)\eta_r \left[1 - \xi_p(\Delta T)\right] A_{pv} \overline{H}_t \\ \Delta T = (T_a - 25°) + C_f (219 + 832 K_{Tm}) \frac{NOCT - 20}{800} \end{cases} \quad (8)$$

with,

$$C_f = \begin{cases} 1 & \text{if} \quad \beta = \beta_{opt} = \psi - \delta \\ 1 - 1{,}17.10^{-4} (s_M - s_r)^2 & \text{else} \end{cases} \quad (9)$$

The parameters NOCT, η_r and ξ_p depend on the type of PV module considered. η_r is the efficiency of the module at the reference temperature of 25°C. ξ_p is the coefficient of temperature, T_a is the average ambient temperature of the month, β_{opt} is the inclination of the PV panel (equal to the latitude minus the solar declination), Normal Operating Cell Temperature (NOCT) is the nominal temperature of the cells in operation. The optimum inclination angle S_M and the actual inclination angle S_r are expressed in degrees. A_{pv} is the surface of the PV panel. The produced energy is reduced by the various losses λ_p and the losses due to the conditioning of the system λ_c.

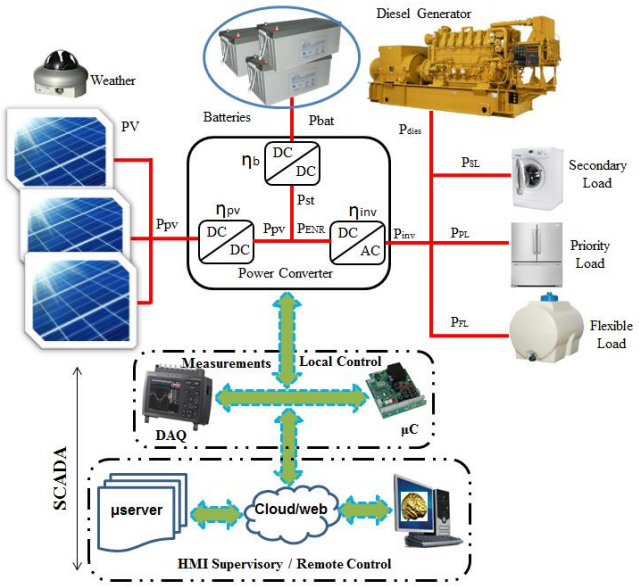

Fig. 3 Synoptic of the microgrid power generation

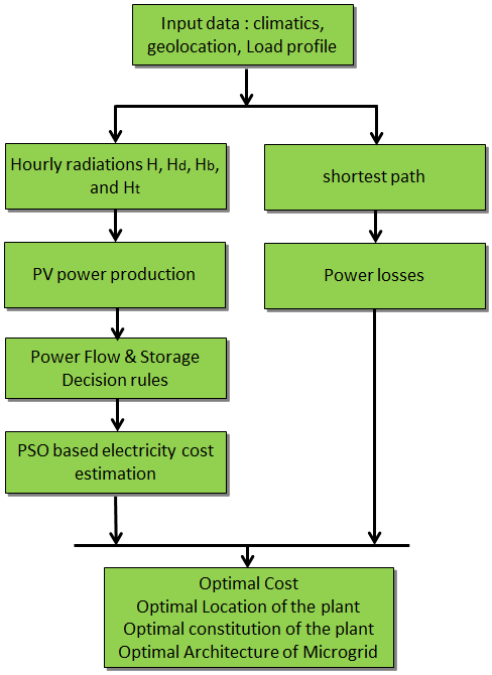

Fig. 4 Flowchart of the optimization process

3.3 Efficiency and Energy Storage Capacity

The Kinetic Battery Model (KiBaM) is used in this study. It is considered as a reservoir of two compartments, one of which contains an immediately available capacity Q_1 (Ah) and the other the "chemically bound" capacity Q_2 (Ah), expressed by (10)[24].

$$\begin{cases} Q = Q_1 + Q_2 \\ Q_1 = Q_{10}e^{-k\Delta t} + \frac{(Qkc+I)(1-e^{-k\Delta t})}{k} + \frac{Ic(k\Delta t-1+e^{-k\Delta t})}{k} \\ Q_2 = Q_{20}e^{-k\Delta t} + Q(1-c)(1-e^{-k\Delta t}) + \frac{I(1-c)(k\Delta t-1+e^{-k\Delta t})}{k} \end{cases} \quad (10)$$

The maximum capacity Q_{max} (Ah) of the battery is defined by (11), for a constant current. In principle, Q_{tc} is estimated from the nominal capacity data and the discharge time indicated by the manufacturer. The maximum energy E_{bmax} (in Wh) is deduced by integrating the instantaneous value of the battery voltage.

$$\begin{cases} Q_{max} = \frac{Q_{tc}(1-e^{-kt_c})(1-c)+ckt_c}{ckt_c} \\ E_{bmax} = V * Q_{max} \end{cases} \quad (11)$$

The maximum values of the current in charge I_{cmaxQ} and discharge I_{dmaxQ} modes are estimated according to the capacities of the battery by (12).

$$\begin{cases} I_{cmaxQ} = \frac{-kcQ_{nom}+kQ_{10}e^{-k\Delta t}+Qkc(1-e^{-k\Delta t})}{1-e^{-k\Delta t}+c(k\Delta t-1+e^{-k\Delta t})} \\ I_{dmaxQ} = \frac{kQ_{10}e^{-k\Delta t}+Qkc(1-e^{-k\Delta t})}{1-e^{-k\Delta t}+c(k\Delta t-1+e^{-k\Delta t})} \end{cases} \quad (12)$$

An additional constraint is taken into account. It consists of defining the limits of the current which determines the internal energy losses through the internal resistance R_{bat}. Indeed, the power delivered or stored by the battery P_{bat} is limited by the power dissipation in the internal resistance according to (13), when considering the discharge mode as the reference. The maximum current is deduced by canceling the derivative of the power.

$$\begin{cases} P_{bat} = E_{bat}I_{bat} - R_bI_{bat}^2 \\ I_{batm} = \frac{V_{bat}}{2R_b} \end{cases} \quad (13)$$

The maximum values to be retained, in charge and discharge modes, correspond to the minimum between the estimated quantities, as presented by (14).

$$\begin{cases} I_{cbmax} = min(I_{cmaxQ}, I_{batm}) \\ I_{dbmax} = min(I_{dmaxQ}, I_{batm}) \end{cases} \quad (14)$$

3.4 Diesel generator fuel consumption et energetic compensation

The hourly consumption of fuel C_{fuel_h} (in liter per hour) of the generator set is a linear function of the nominal power P_{ndies} (kW) and that delivered in operation P_{dies} (kW) (15). The powers delivered vary according to the hourly demand. The cumulative over 8760 h is the annual fuel consumption C_{fuel_a}.

$$\begin{cases} C_{fuel\_h} = B * P_{ndies} + A * P_{dies} \\ C_{fuel\_a} = \sum_{h=1}^{8760} C_{fuel\_h} \end{cases} \quad (15)$$

The coefficients are defined by A= 0,246l/kWh and B=0,08415l/kWh [25].

4. Estimation of the Optimal Cost of Electricity

The effective annual interest rate T_r is estimated according to the nominal discount rate T_n and the expected inflation rate t_{inf}. The Capital Recovery Factor (CRF) is expressed by (16) for the project's lifetime, corresponding to the PV lifetime N_{pv}, in this study.

$$\begin{cases} T_r = \frac{T_n - t_{inf}}{T_n + t_{inf}} \\ CRF = \frac{T_r(1+T_r)^{Npv}}{(1+T_r)^{Npv}-1} \end{cases} \quad (16)$$

The Total Life Cycle Cost *TLCC* os the system is defined by (17) as the sum of the total costs (in €/ year) of investment CTA_{inv}, of component replacement CTA_{remp}, of maintenance $CTA_{o\&m}$ and of residual value *VR* at the end of the lifetime. *VR* is considered as null, in general case.

$$TLCC = CTA_{inv} + CTA_{remp} + CTA_{o\&m} + VR \quad (17)$$

Let's define $E_{conso}(h)$ as the hourly energy consumption, in kWh, by all users over the year. The cost of electricity C_{kwh}, in *€/kWh*, is obtained from the ratio (18). The annualized cost of the system CCVA (in € / year) is estimated from (18) [26], [27].

$$\begin{cases} \min C_{kwh} = \frac{CCVA}{\sum_{h=1}^{8760} E_{conso}(h)} \\ CCVA = \text{TLCC} * CRF \end{cases} \quad (18)$$

To estimate the discounted costs of the components, the Present Value Factor $PVF_{a,x}$ [28] is used to convert, or conversely, the Future Cost (*FC*) of a monetary sum, that it is about incomes or costs, with its present value defined by (19), for *n* years. The investment cost CTA_{inv} (20) includes acquisition costs of PV panels, batteries and generators as well as the interfaces and electronic converters.

$$\begin{cases} CA_{a,x} = FC_{a,x} * FVA_{a,x} \\ PVF_{a,x} = \frac{1}{(1+T_{ar,x})^{Nx}} \end{cases} \quad (19)$$

Because of the investment is made today, $CF_{a,x}$=$CA_{a,x}$, an uniform factor for all components can be used, such as $FVA_{inv,x}$=1. N_x is defined as the number of component *x*.

$$CTA_{inv} = \begin{matrix} N_{pv} \cdot CA_{I,pv} + N_{dies} \cdot CA_{I,dies} + \cdots \\ +N_{bat} \cdot CA_{I,bat} + N_{conv} \cdot CA_{I,conv} \end{matrix} \quad (20)$$

The total discounted replacement cost CTA_{remp}(€) of the components (batteries, converters) is defined by (21), with $C_{r,x}$ the replacement cost of the unit considered. It is considered that this cost is equal to the current acquisition cost $CA_{inv,x}$ of the same unit. Let N_x be the number of time the component *x* is replaced during the lifetime. This is the ratio between the lifetime of the overall system and the component replacement period.

$$\begin{cases} CTA_{remp} = \tau_{bat,r} + \tau_{conv,r} \\ \xi_x = entier\left(\frac{N_{pv}}{N_x}\right) \end{cases} \quad (21)$$

With,

$$\begin{cases} \tau_{bat,r} = \xi_{bat} * N_{bat} \cdot FC_{inv,bat} * PVF_{remp,bat} \\ \tau_{conv,r} = \xi_{conv} * N_{conv} \cdot FC_{I,conv} * PVF_{remp,conv} \end{cases} \quad (22)$$

The total cost of maintenance $CTA_{o\&m}$(€) is expressed by (23)

$$CTA_{o\&m} = \tau_{o\&m,pv} + \tau_{o\&m,dies} + \tau_{o\&m,bat} + \tau_{o\&m,bat} \quad (23)$$

With,

$$\begin{cases} \tau_{o\&m,pv} = N_{pv} * FC_{o\&m,pv} * FVA_{o\&m,pv} \\ \tau_{o\&m,dies} = N_{dies} * FC_{o\&m,dies} * FVA_{o\&m,dies} \\ \tau_{o\&m,bat} = N_{bat} * FC_{o\&m,bat} * FVA_{o\&m,bat} \\ \tau_{o\&m,conv} = N_{conv} * FC_{o\&m,conv} * FVA_{o\&m,conv} \end{cases} \quad (24)$$

But, when considering an average annual maintenance cost $CM_{o\&m}$ of the overall system, $CTA_{o\&m}$ cost can be expressed as (25).

$$CTA_{o\&m} = N_{pv} * CM_{o\&m} * FVA_{o\&m} \quad (25)$$

The expected cost of electricity C_{kwh} is the minimum cost to make operating expenses as well as the recovery of the investment costs, with zero profit. By incorporating an expected profit corresponding to a percentage of the investment cost, the price of electricity may increase. The objective function aims to minimize this cost by applying a multi-criteria optimization method based on particle swarm behavior.

5. Strategy of power flow management

In a renewable energy system, the batteries support a relative variability of production and consumption, to achieve a power balance on the AC bus as (26).

$$\begin{cases} \sum_{i=1}^{n} P_i(t) = 0 \\ \eta_{inv} * \left(P_{pv}(t) - P_{st}(t)\right) + P_{dies}(t) - P_{Load}(t) = 0 \end{cases} \quad (26)$$

The nominal power of the load consists of two components. These are the priority and secondary loads, as expressed by (27). A degree of freedom is defined by the so-called Flexible Load P_{FL} which value is zero in normal operation. It corresponds to a variable and unpredictable load.

$$P_{Load}(t) = P_{PL}(t) + P_{SL}(t) \quad (27)$$

The powers provided by the PV and battery to the AC bus are expressed by (28).

$$\begin{cases} P_{pv_{AC}}(t) = \eta_{inv} * P_{pv}(t) \\ P_{st\_AC}(t) = \eta_{inv} * P_{st}(t) \end{cases} \quad (28)$$

On the other hand, the actual contribution of the PV, $Contrib_{pv}$, at a given moment can be lower than the PV production at the same time, due to the losses and the storage processes. Since the batteries are intended to absorb exclusively additional PV production, the instantaneous contributions of renewable energy productions on the DC and AC buses can be expressed according to (27).

$$\begin{cases} P_{enr\_AC}(t) = P_{pv\_AC}(t) - P_{st\_AC(t)} \\ P_{enr\_DC}(t) = P_{pv}(t) - P_{st}(t) \end{cases} \quad (27)$$

Energy flow management is based on sequential tests, the first level is defined by the difference (28) between photovoltaic production and the load demand. $Potential_{st}$ and $Deficit_{dst}$ are defined as the power that can be stored, or discharged, by the batteries, respectively.

$$\begin{cases} \Delta P_{prod}(t) = P_{pv\_AC}(t) - P_{Load}(t) \\ Potential_{st}(t) = \frac{\Delta P_{prod}(t)>0}{\eta_{inv}*\eta_{bat}} \\ Deficit_{dst}(t) = \frac{\Delta P_{prod}(t)<0}{\eta_{inv}*\eta_{bat}} \end{cases} \quad (28)$$

The system's operation can be illustrated by several scenarios determined by the energy availability and the state of the batteries charge, as well as the level of the energy demand. The energy deficit is compensated by the diesel generator that can operate in continuous or intermittent mode, with power and speed limits. The operating dynamics have an impact on the overall cost, through the size of the system and the maintenance costs. In the limited operation range, the diesel generator can provide variable power between the extrema, in aims to improve its lifetime.

The charge and discharge capacity of the battery is estimated from the EDC as (29).

$$\begin{cases} \Delta E_{dbat} = E_{bat}(t-1) - E_{bat\_min}(t) \\ \Delta E_{cbat} = E_{bat\_max}(t) - E_{bat}(t-1) \end{cases} \quad (29)$$

The PV contribution is equal to the demand of the load as (30).

$$\begin{cases} Contrib_{pv}(t) = P_{Load}(t) \\ GAP_{ch} = \Delta E_{cbat} - Potential_{st}(t) \\ Gap_{dech} = \Delta E_{dbat} - |Deficit_{dst}(t)| \end{cases} \quad (30)$$

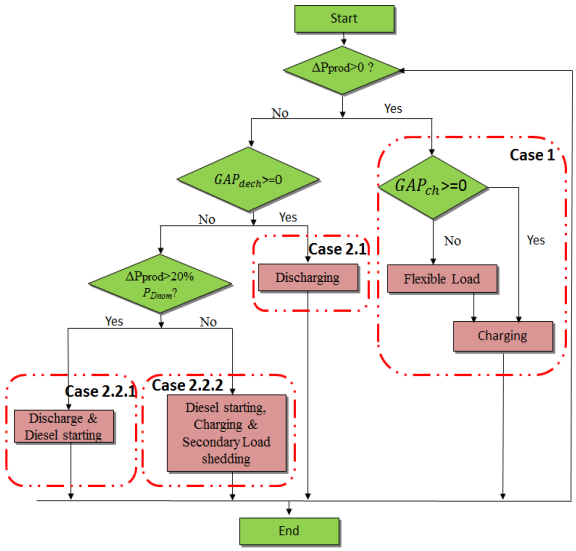

Fig. 5 Principle algorithm of energy flow management in the multisource system

Fig.5 describes the main cases identified in the distribution of energy flow in the multisource system. These cases are used in the energy management algorithm for system sizing. The generator set is considered in intermittent operation with imposed power limits and the PV outputs are optimized by the maximum power point tracking method. In (*Case 1*), the PV production is greater than the demand of the load, and lower in Case 2. Photovoltaic energy is insufficient to satisfy all the needs of the electrical loads. The batteries can be used to compensate the energy deficit. If necessary, the diesel group will be involved. If the battery is sufficient to compensate the deficit, (*Case 2.1*) occurs, otherwise, the battery is insufficient to compensate the deficit and the Diesel can be started (*Case 2.2*). The minimum power delivered by the diesel must be greater than or equal to 20% of its nominal power. (*Case 2.2.2*) occurs if the deficit is greater than the batteries capacity, and less than the minimum starting power of the diesel generator. So, the batteries can be charged and the flexible charge activated if necessary. Else, the loop of (*Case 2.2.1*) starts.The algorithm of energy management is implemented in Matlab software and called by the Particle Swarm Optimization (PSO) method during the system sizing simulations. The optimal combination of the system components (PV panels, diesel generator, batteries) is estimated by taking into account the various constraints identified in order to minimize the objective function. In this case study, it consists to minimize the cost of electricity C_{kwh}.

1) Particle Swarm Optimization (PSO) Method

The Particle Swarm Optimization (PSO) method was originally proposed by R. C. Eberhart and J. Kennedy in 1995 [29]-[33]. It is inspired from the dynamics of the social behaviour of animals moving in compact groups (bee swarms, group flights of birds …). The probability of an individual's decision is based on social and community behaviour. At each simulation step, the velocity and position of each particle are updated and they retain in memory their coordinates associated with the best solution (physical condition) it has reached so far. This is the best personal solution called P_{best}. But, the overall solution found corresponds to the best overall value G_{best}, and its coordinates, obtained so far by any particle of the population. The particle speed is weighted with randomly generated numbers to accelerate the particle to the strongest and most generous locations. From the initial version of the PSO algorithm, some improvements are made by the some authors. Part of them proposed by [29], [30] use an additional coefficient called "constriction coefficient" which improves the convergence of the particles and prevents the collapse if the adequate social conditions are reached.

The PSO algorithm, which is simple to understand, to program and to use, is particularly effective for continuous variable optimization problems. The advantage of the PSO is its insensitivity to the scaling of design variables, its simple implementation, its ease of paralleling for simultaneous processing, and its lack of derivatives. It is also an algorithm that uses very few parameters and whose global search is very efficient. However, like all metaheuristics, the PSO has disadvantages, which still repel some users. The problem of premature convergence, which can lead algorithms of this type to stagnate in a local optimum, is one of these disadvantages.

As part of this study, the algorithm is applied to energy data under defined constraints and assigned objectives. From the community energy needs, the optimization criteria are defined and applied to the identified variables of the system sizing models. In addition, the constraints and the objective function are formulated. Different scenarios corresponding to various configurations of the microgrid plant are tested in iterative processes. Then, the optimal solution of the shortest path between all villages is chosen. The PSO algorithm is based on the speed $V_i^{(t+1)}$ (31) of the individual *i* at the iteration (*t+1*) related to the acceleration coefficients C_1 and C_2 which are random binary numbers [0, 1], on the position X_i^t of the individual *i* at the iteration *t*, on the best individual position P_{best} at the iteration *t*, and on the best global position G_{best} until the iteration *t*.

$$\begin{cases} V_i^{t+1} = K[V_i^t + \gamma_i^t + \beta_i^t] \\ X_i^{t+1} = X_i^t + V_i^{t+1} \end{cases} \quad (31)$$

with,

$$\begin{cases} \gamma_i^t = c_1 r_1 (Pbest_i^t - X_i^t) \\ \beta_i^t = c_2 r_2 (Gbest_i^t - X_i^t) \end{cases} \quad (32)$$

The relationships between the constriction coefficients are defined by (33).

$$K = \frac{2}{\left|2-\varphi-\sqrt{\varphi^2-4\varphi}\right|} \ , \varphi = c_1 + c_2, \varphi > 4 \quad (33)$$

For good convergence, the condition (φ> 4) on the constriction factor is verified by the choice of coefficients $C_1 = C_2 = 2.05$ [30].

B. Results of experimental validation of the energy management strategy

The storage device is supervised by Battery Management System (BMS) that integrates the main theoretical limits of the battery from the current point of view, charging/discharging capacity and extreme temperature levels. Likewise, each cell is monitored to prevent an imbalance that can affect the proper operation of the system. The estimated limits of currents and capacities are implemented to the supervisory algorithm.

Experimental tests were conducted to test the energy management and decision laws that are implemented under the python language on the programmable automate associated to a webserver. The experimental platform shown in Fig.6 consists of PV panels (2.5kW$_p$), Li-Ion batteries (5kWh), electrical load (4kW), and a multifunctional inverter (5kW). The DC input voltage range of the inverter varies between 120V and 500V with an AC output of 230V/50Hz. A data acquisition and control system (SCADA) is used for remote management to process in real time a large number of data through webserver.

Fig.6 Experimental test platform of multi-sources power plant.

The energy management system of the microgrid allows local or remote control of technical installations (sensor networks, centralized technical management. It is a solution for simple and fast operation from any client station equipped with an internet browser. Fig.7 shows the temporal variations of the PV productions and the profile of the main load. High variability is observed due to the fairly frequent passage of clouds during the test period. Scaled variations are imposed to the load to better observe and analyze flow dynamics. The proposed energy management strategy defines two categories of electrical loads: a main load P_{PL} (sum of priority and secondary loads) as well as a flexible load P_{FL} that is powered based on the energy availability. This last can be a pumping system, watering, slippery loads on the day (dishes, laundry ...). Given the constraints of using a diesel generator in the laboratory, a connection to the electrical network is made. The excess energy for the flexible loads P_{FL} is sent to the grid and the expected contribution of the generator is provided by the power grid. The curve of the PV power as a function of the PV voltage, Fig.8, shows that the operation is maintained at the maximum power regardless of the variation of the solar radiation. This illustrates the effectiveness of the implemented MPPT method. The batteries processes of charging and discharge are presented in Fig.9, with the power of flexible loads and diesel emulator ones. Fig.10 shows the performance of the system regulation through the voltages evolutions of the solar panels and the AC bus. The ripples of the PV voltage are limited in a narrow band around the average value due to good regulation. The batteries charge and discharge processes depend on the relative variations of PV output and load demand. In the case of a complete charge of batteries, the surplus of PV energy is returned to the grid, it is the part of energy allocated to the flexible loads. The contribution of the diesel generator is assimilated to the phase during which the electric grid supplies power.

6. Optimal Power Plant Design and Location

Particle swarm optimization is used to determine the size of the system as well as the characteristics of the components. The main objective is to minimize the cost of electricity produced and consumed in the microgrid. But, because of the need to install power transmission lines, losses of power are predictable. These must be taken into account in the definition of the architecture of the microgrid whose interconnections must realize the minimum of possible losses.

Once the architecture is estimated, the plant location must also achieve the minimum losses and/or the cost of electricity compared to other target villages. The ideal case would be to achieve the minimum of the two objectives on the same village but, in the present study, the estimation of the two parameters is done independently. This nonetheless opens the way to perspectives of combining the two approaches. The final arbitration for choosing the optimal location is done by comparing the results of the two approaches.

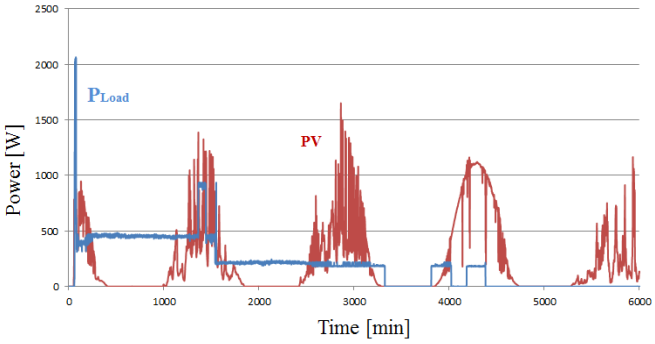

Fig.7 Temporal variations of PV productions and power of the main load

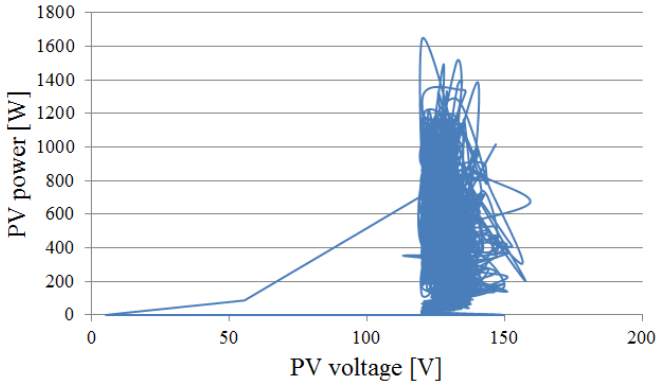

Fig.8 : PV power as a function of voltage, highlighting the MPPT performance

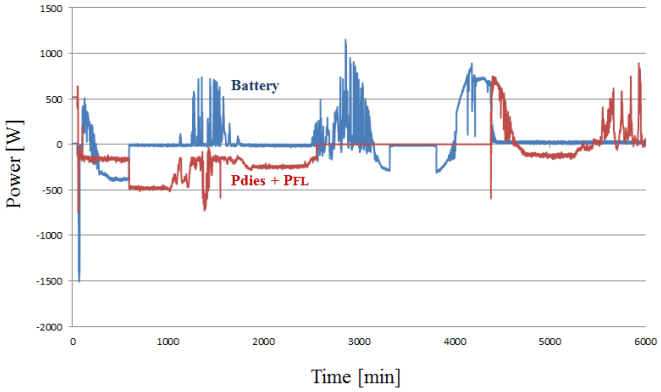

Fig.9 : Charging power and discharge the battery (blue) and power flexible loads (red, negative) and provided by the emulator of the diesel group (red, positive).

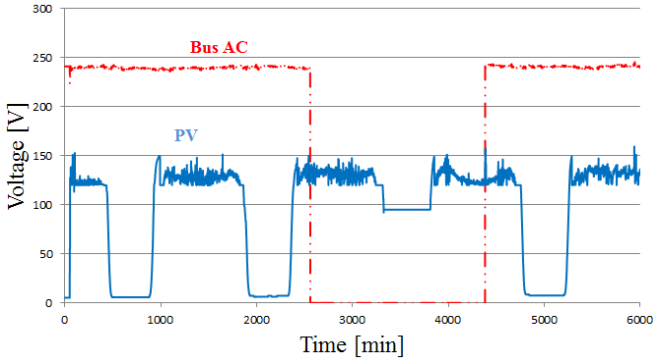

Fig. 10: Voltages variations of the PV and AC bus

A. Method of the Minimum Lines Losses

The shortest path between villages is generated by applying the Prim's algorithm to the distances matrix. The goal is to find the minimum spanning tree. The matrix of the shortest paths between the villages is presented in Table 2. It defines the architecture of the microgrid. But, it is necessary to find the optimal location of the power generation plant.

The microgrid is defined by a 20kV transmission and a 0.4kV distribution lines. The power losses in the transmission lines are estimated by considering each village, successively, as the location of the generation plant. Simulation results are presented in Table 3. The daily energy consumption in the eight villages is estimated around 5.6MWh. The lowest ratio of energy losses is estimated around 5.69% of the daily energy. It corresponds to the village 7 which seems to be a suitable location of the generation plant. This can ensure a lower energy flow in the transmission lines because of a big part of energy is consumed at village 7.

Table 2. Matrix of the shortest path between villages i and j

Village i	Village i	Distance (km)
1	2	11.45
1	4	18.89
1	3	27.5
3	6	17.46
4	7	47.56
7	8	27.05
7	5	40.61

Table 3. Power losses estimated for each village taken as the power plant location

Village	Demand (kWh)	∑Losses (kWh)	Ratio (%)
1	63.29	707.66	12.64
2	916.52	814.20	14.54
3	413.15	1034.11	18.47
4	956.30	547.40	9.78
5	768.65	736.65	13.16
6	168.92	1253.34	22.39
7	1829.08	318.33	5.69
8	483.36	635.71	11.35

B. Method of the Minimum Cost Of Electricity (COE)

In this method, climatic data of each village are used to estimate the PV power productions, the storage capacity and the diesel generator contributions, according to the total energy demand in the microgrid. The minimum cost of electricity is reached by applying the PSO algorithm. For each village, considered as the location of the power generation system, the minimum of the COE is found from iterative simulations. This is called local minimum. For each case, size and nature of the system components are proposed and presented in Fig.11. Relationship between components can be observed. The solar radiation value has a strong influence on the PV output, and consequently, on the transit power which determines the size of the converters.

At the end of all simulations, the global minimum is reached and it defines the optimal price of electricity. So, the corresponding village can be considered as the optimal location of the power plant. In this case, village 6 provides the minimum COE of 0.108 euros, as presented in Table 4. It achieves the best compromise in terms of PV production, satisfaction of energy demands, storage, diesel generator size and loss of loads.

C. Optimal location of the power plant

Depending on the considered optimization criterion, it is possible to achieve different results concerning the optimal village to be retained for the implementation of the power sources. In the case study, villages 6 and 7 present minimum cost and power loss respectively. An additional parameter of decision support is necessary to choose the suitable location. It can be based on the estimation of the total cost of the energy production and the lines losses ones, as in Table 4. The architecture of the microgrid presented in Fig. 12, with the power plant located at village 6. It can be observed that

the village 6 has the lowest total COE, one of the lowest energy consumption but presents the great loss of power when it is considered as the location of power plant. While village 7 has the largest consumption ratio and the lowest power loss. In addition, it has more solar potential than village 6.

7. Conclusion

The Multi-village microgrid aims to ensure the energy autonomy of several neighboring villages in a system of energy cooperation through their interconnection. The system proposed in this study integrates PV panels, storage battery, diesel generator and different kind of loads. Such a combination strengthens energy availability with a significant renewable energy penetration rate but requires dedicated sizing based on efficient sizing models, based on experimental characterizations, behavioral analysis and definition of management strategies. The energy management in the system is based on decision rules.

The proposed methodology for the design of such a system is described by the following main steps:

- development of a mathematical model for estimating the solar potential of a village, as a function of optimal inclination, direction and position;
- modeling of power sources (PV, generator) and storage batteries, for the purpose of estimating the producible and the constituents of the power plant;
- development of a methodological approach for estimating energy needs by sector of activity and services for each village;

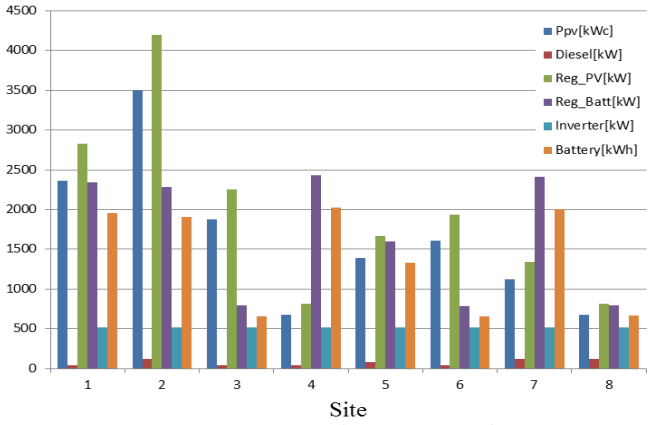

Fig.11 Optimal constitution of the power plant for each village considered as the system location. Size of PV, Diesel generator, PV converter (Reg_PV), batteries, battery converter (Reg_Batt), and inverter are presented in kW and kWh (for battery).

Table 4: Estimation of the COE, energy losses and cost of the total production of electricity.

Village	COE €/kWh	Energy Need kWh	Lines losses		Cost Of energy €		
			Energy kWh	Ratio (%)	Useful	lost	Total
1	0,158	5600	117,94	2,06	884,8	18,635	903,435
2	0,2	5600	135,7	2,37	1120	27,14	1147,14
3	0,14	5600	172,35	2,99	784	24,129	808,129
4	0,155	5600	91,23	1,6	868	14,141	882,141
5	0,164	5600	122,78	2,15	918,4	20,135	938,535
6	0,108	5600	208,89	3,6	604,8	22,56	627,36
7	0,187	5600	53,05	0,94	1047,2	9,921	1057,121
8	0,13	5600	105,95	1,86	728	13,774	741,774

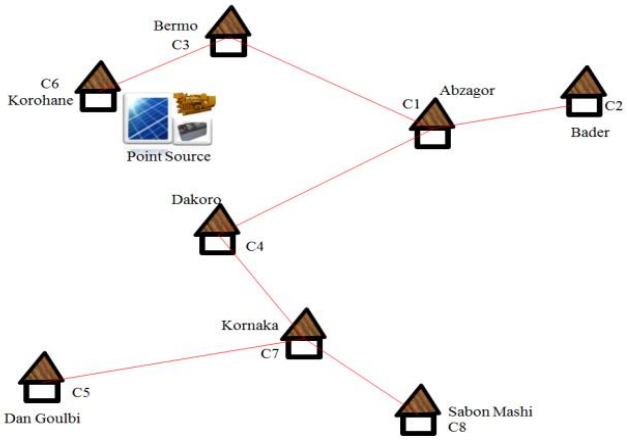

Fig. 12 Optimal location of the power plant and the architecture of the microgrid.

- analysis of the energy efficiency and power losses;
- study of the possible architectures of the microgrid and estimation of the shortest path based on the graph theory;
- Estimation of the optimal location of the power plant by minimizing the cost of electricity as well as losses of power by using the particle swarm optimization method;
- Development of energy management algorithms and decision support in a multi-source system;

The analysis of the results obtained shows a real maximization of the PV production as well as the good performance of control and the overall supervision.

References

[1] A. Brew-Hammond, "Energy access in Africa: Challenges ahead", Energy Policy, vol. 38, no 5, p. 2291-2301, 2010.

[2] F. M. Butera, P. Caputo, R. S. Adhikari, et A. Facchini, "Urban Development and Energy Access in Informal Settlements. A Review for Latin America and Africa", Procedia Eng., vol. 161, p. 2093‑2099, 2016.

[3] C. K. Pandey et A. K. Katiyar, "A note on diffuse solar radiation on a tilted surface", Energy, vol. 34, no 11, p. 1764‑1769, 2009.

[4] F. Besharat, A. A. Dehghan, et A. R. Faghih, "Empirical models for estimating global solar radiation: A review and case study", Renew. Sustain. Energy Rev., vol. 21, p. 798‑821, 2013.

[5] A. Adell, "Determination of the optimum inclination of a flat solar collector in function of latitude and local climatic data", Revue Physique Appliquee, vol. 17, no 9, p. 569‑576, 1982.

[6] M. M. El-Kassaby, "Monthly and daily optimum tilt angle for south facing solar collectors; theoretical model, experimental and empirical correlations", Sol. Wind Technol., vol. 5, no 6, p. 589‑596, janv. 1988.

[7] S. A. Khalil, A. M. Shaffie, "A comparative study of total, direct and diffuse solar irradiance by using different models on horizontal and inclined surfaces for Cairo, Egypt", Renew. Sustain. Energy Rev., vol. 27, p. 853‑863, 2013.

[8] R. Tang, T. Wu, « Optimal tilt-angles for solar collectors used in China », Appl. Energy, vol. 79, no 3, p. 239‑248, 2004.

[9] G. Notton, P. Poggi, C. Cristofari, "Predicting hourly solar irradiations on inclined surfaces based on the horizontal measurements: Performances of the association of well-known mathematical models", Energy Convers. Manag., vol. 47, no 13–14, p. 1816‑1829, 2006.

[10] C. A. Gueymard, "Direct and indirect uncertainties in the prediction of tilted irradiance for solar engineering applications", Sol. Energy, vol. 83, no 3, p. 432‑444, 2009.

[11] H. Darhmaoui, D. Lahjouji, "Latitude Based Model for Tilt Angle Optimization for Solar Collectors in the Mediterranean Region", Energy Procedia, vol. 42, p. 426‑435, 2013.

[12] G. A. Kamali, I. Moradi, A. Khalili, "Estimating solar radiation on tilted surfaces with various orientations: a study case in Karaj", Theor. Appl. Climatol., vol. 84, no 4, p. 235‑241, 2006.

[13] D. G. Erbs, S. A. Klein, J. A. Duffie, "Estimation of the diffuse radiation fraction for hourly, daily and monthly-average global radiation", Sol. Energy, vol. 28, no 4, p. 293‑302, 1982.

[14] J. K. Yohanna, I. N. Itodo, V. I. Umogbai, "A model for determining the global solar radiation for Makurdi, Nigeria", Renew. Energy, vol. 36, no 7, p. 1989‑1992, 2011.

[15] A. M. Muzathik, M. Z. Ibrahim, K. B. Samo, W. B. Wan Nik, "Estimation of global solar irradiation on horizontal and inclined surfaces based on the horizontal measurements", Energy, vol. 36, no 2, p. 812‑818, 2011.

[16] O. O. Ajayi, O. D. Ohijeagbon, C. E. Nwadialo, and O. Olasope, "New model to estimate daily global solar radiation over Nigeria", Sustain. Energy Technol. Assess., vol. 5, p. 28‑36, 2014.

[17] Y.-P. Chang, "Optimal the tilt angles for photovoltaic modules in Taiwan", Int. Journal of Electr. Power Energy Syst., vol. 32, no 9, p. 956‑964, 2010.

[18] K. Bakirci, "General models for optimum tilt angles of solar panels: Turkey case study", Renew. Sustain. Energy Rev., vol. 16, no 8, p. 6149‑6159, 2012.

[19] M. David, P. Lauret, J. Boland, "Evaluating tilted plane models for solar radiation using comprehensive testing procedures, at a southern hemisphere location", Renew. Energy, vol. 51, p. 124‑131, 2013.

[20] K. Skeiker, "Optimum tilt angle and orientation for solar collectors in Syria", Energy Convers. Manag., vol. 50, no 9, p. 2439‑2448, 2009.

[21] A. P. de Souza, J. F. Escobedo, "Estimates of hourly diffuse radiation on tilted surfaces in Southeast of Brazil", Int. J. Renew. Energy Res. IJRER, vol. 3, no 1, p. 207‑221, 2013.

[22] D. G. Erbs, S. A. Klein, J. A. Duffie, "Estimation of the diffuse radiation fraction for hourly, daily and monthly-average global radiation", Sol. Energy, vol. 28, no 4, p. 293‑302, 1982.

[23] Y. Sokona, Y. Mulugetta, H. Gujba, "Widening energy access in Africa: Towards energy transition", Energy Policy, vol. 47, p. 3‑10, 2012.

[24] J. F. Manwell *et al.*, "hybrid2- A Hybrid System Simulation Model - Theory Manual", Renewable Energy Research Laboratory, University Of Massachusetts, June 2006, 2006.

[25] R. Dufo-López, J. L. Bernal-Agustín, "Multi-objective design of PV–wind–diesel–hydrogen–battery systems", Renew Energy Journal, vol. 33, no 12, p. 2559‑2572, 2008.

[26] W. Short, D. J. Packey, T. Holt, "A manual for the economic evaluation of energy efficiency and renewable energy technologies", NREL/TP--462-5173, 35391, mars 1995.

[27] U. Aswathanarayana, T. Harikrishnan, K. M. Thayyib Sahini, "Green energy: technology, economics, and policy", CRC Press, 2010.

[28] B. Agrawal, G. N. Tiwari, "Building integrated photovoltaic thermal systems: for sustainable developments", Cambridge, UK 2011.

[29] M. Clerc, J. Kennedy, "The particle swarm - explosion, stability, and convergence in a multidimensional complex space", IEEE Trans. Evol. Comput., vol. 6, no 1, p. 58‑73, 2002.

[30] M. Clerc, "Particle swarm optimization", ISTE, London 2006.

[31] S. Y. Lim, M. Montakhab, H. Nouri, "A constriction factor based particle swarm optimization for economic dispatch", In Proceedings of European Simulation and Modelling Conference, UK 2009.

[32] S. Sengupta, A. K. Das, "Particle Swarm Optimization based incremental classifier design for rice disease prediction", Comput. Electron. Agric., vol. 140, p. 443‑451, 2017.

[33] L. Idoumghar, D. Fodorean, A. Miraoui, "Using hybrid Constricted Particles Swarm and simulated annealing algorithm for electric motor design", 2010.